JOURNAL OF MATERIALS SCIENCE **34** (1999) 365–369

Sequential electron beam evaporation of YBCO thin films through the barium fluoride route

V. H. S. MOORTHY, V. S. TOMAR
Superconductivity group, National Physical Laboratory, New Delhi 110 012, India
E-mail: vhsm@physics.iisc.ernet.in

Superconducting YBCO thin films have been fabricated by sequential electron beam evaporation of metallic constituents for yttrium and copper while barium is replaced with BaF_2. The conversion of $BaF_2 \rightarrow BaO$ has been attained through wet oxygen annealing. Correlations of stoichiometry with microstructural, as well as superconducting, properties of the films have been examined. Results are given for $YBa_2Cu_3O_{7-\delta}$ thin films on $SrTiO_3$ (1 0 0) and YSZ (1 0 0) single crystal substrates. The usefulness of the BaF_2 preparation route for the fabrication of mixed phase (Y123 + Y124) and pure Y124 is also demonstrated. Microstructural properties of Y123 thin films indicate different growth processes for the two substrates. © *1999 Kluwer Academic Publishers*

1. Introduction

The thin-film synthesis of high T_c superconductor (HTS) materials is a key technology for application in electronic devices and their integration with semiconductor electronics. The HTS materials have been grown by metal evaporation [1], sputtering [2], laser ablation [3] and metalorganic chemical vapour deposition (MOCVD) [4]. *In situ* processes (both for deposition and annealing) have already resulted in thin films with good structural and superconducting characteristics. However, if similar quality can be attained through *ex situ* annealing it would be more convenient and useful for device fabrication. This can be accomplished [5] with the use of BaF_2 as a source material, which has been shown to reduce greatly the sensitivity of as-deposited films to fabrication and environmental conditions.

The selection of substrates for epitaxial growth of YBCO films needs to satisfy several requirements [6]. In this paper we report the growth of YBCO superconducting thin films on $SrTiO_3$ (1 0 0) and YSZ (1 0 0) single crystal substrates using sequential electron beam evaporation of Yttrium, BaF_2 and copper, followed by an optimized wet and dry annealing procedure. Various thin-film parameters have direct bearing on stoichiometry, crystallite size and superconducting transition temperature. The crystal structure and microstructural studies are also reported.

2. Experimental procedure

An ultra-high vacuum (UHV) system (Varian VT118) equipped with 10 kV electron gun with three crucibles was used for the fabrication of thin films. A vacuum better than 5.0×10^{-8} mbar was obtained in a reasonable time by the judicious use of a turbo molecular pump, a sputter getter ion pump and a titanium sublimation pump. The substrates (cleaned and well-polished single-crystal $SrTiO_3$ (1 0 0) were mounted 30 cm above the evaporating source on the heater-substrate holder. The substrates were heated to 600 °C for about 1 h in good vacuum to attain cleaning from volatile impurities. The evaporating source materials–yttrium (99.999%), BaF_2 (99.9%) and copper (99.99%) –were thoroughly degased by focusing and rastering the electron-beam such that on heating and melting of the materials, the vacuum in the chamber remained stable.

The thickness of the film of each material was estimated by considering the density and molecular weight of the materials, such that on evaporation, the metal stoichiometric ratio was close to $Y : BaF_2 : Cu :: 1 : 2 : 3$. The evaporation of the individual materials was monitored and controlled by microprocessor-controlled quartz crystal thickness monitor (Intellemetrics IL 400). The thickness measurement through the quartz crystal involved density, D, acoustic impedence, Z, and a geometrical factor of the system, called a tooling factor. The tooling factor is defined as the ratio of the thickness measured by the quartz crystal to the actual thickness measured by the stylus technique, keeping the evaporation geometry constant. Thus, the tooling for a material is determined by evaporating a known thickness (0.1 μm) as determined by the quartz crystal and measuring the same thickness by the stylus measurement method. While determining the tooling factor, the evaporation parameters (geometry of the evaporation arrangement, degasing procedures, vacuum during evaporation) were kept unchanged. The tooling factors for each material were thus determined by the interative method such that the observed thickness of the deposited film was nearly equal to the measured thickness. The tooling factors for yttrium, BaF_2 and copper were determined separately.

The evaporation of the materials (yttrium = 18.04 nm, $BaF_2 = 63.15$ nm, copper = 18.79 nm) in order to obtain the 1 : 2 : 3 metallic ratio was carried

TABLE I Deposition parameters

Parameter	Value
Substrate	$SrTiO_3$ (1 0 0)/YSZ (1 0 0)
Source substrate distance	30 cm
Substrate temperature	600 °C
Vacuum during deposition	3.0×10^7 mbar
Deposition rate	0.1 nm
Tooling	
Yttrium	1.688
BaF_2	1.165
Cu	1.043
Thickness	
Yttrium	18.04 nm
BaF_2	63.15 nm
Cu	18.79 nm
Total thickness	Typically 0.5–1 μm

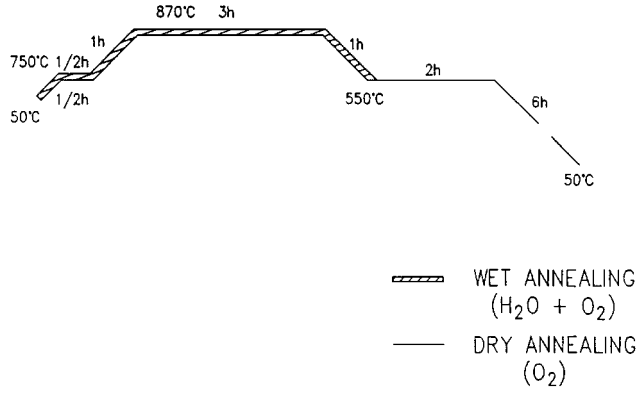

Figure 1 Schedule for *ex situ* annealing treatment given to the films fabricated through the BaF_2 route.

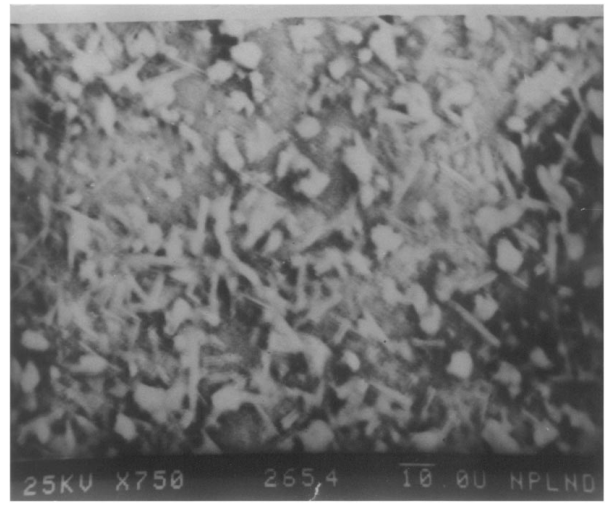

Figure 2 Scanning electron micrograph of typical yttrium-rich YBCO thin film. Needle-like structures may be noticed.

out by considering the density, the acoustic impedence from the standard tables [7], and the tooling factors determined experimentally. The conditions (summarized in Table I) of evaporation were maintained the same as those for determining the tooling factors. Thus, the fabrication of yttrium, BaF_2 and copper stakes of films 100 nm thick was carried out in five batches, such that the total thickness obtained was typically of the order of 500 nm.

The as-deposited films were amorphous and shiny. They were insulating and thus had very high room-temperature resistivity. Several transformations take place in the film in order to convert it into a superconductor with good structural properties. In the first step, the BaF_2 is converted to BaO followed by a second step involving the formation of YBCO with orthorhombic structural properties, and finally the desired oxygenation of YBCO to attain optimum superconducting properties. In the usual annealing procedure [9] first the sample is heated to 750 °C where it is observed that BaF_2 dissociates in the presence of wet oxygen ($H_2O + O_2$) followed by the second stage, where the temperature is raised to 850–900 °C which facilitates development of proper morphology together with the formation of YBCO. Finally, the temperature is lowered to approximately 500 °C in order to facilitate the desired oxygenation of the samples.

The annealing schedule followed in the present work is shown in Fig. 1. The temperature and the duration of each step was varied in order to obtain films with optimum superconducting properties. The duration of the wet oxygenation was also varied. The microstructure was studied by scanning electron microscopy (SEM) (Jeol-JSM35C scanning microscope) and the phase purity was identified by XRD using the CuK_α line (Siemens D-500 X-ray diffractometer).

3. Results and discussion

3.1. Properties of off-stoichiometric films: colour of films and microstructure

The deleterious effects of off-stoichiometry of metals over the superconducting properties of YBCO thin films are well known [9]. Various stages of the formation of YBCO have been characterized and monitored through resistivity-temperature (R-T), SEM studies. The formation of YBCO compound in accordance with the equilibrium phase diagram [10] needs optimum temperature, pressure and annealing treatments. It is possible to estimate the quality of the samples through visible observation of the colour and microstructure as evidenced by scanning electron microscope (SEM). The green colour of the samples indicates insufficient oxygenation and growth of insulating phase (green phase). Electrical measurements on these films show semiconducting properties. The scanning electron micrograph (Fig. 2) shows the presence of needle-like precipitates.

The films with excess copper (over the stoichiometric composition) have large room-temperature resistivity (approximately a few kΩ) causing the R-T measurements to be sensitive to noise and the films are found to be insulating. The scanning electron micrographs (Fig. 3) show white conglomerates indicating the formation of insulating copper oxide.

The annealed samples are whitish in colour. Repetitive annealing with increased durations of high-temperature annealing fail to convert the whitish colour to the dark-brown phase. This behaviour is attributed to excessive barium content. There are several well known problems [11] in the case of such films.

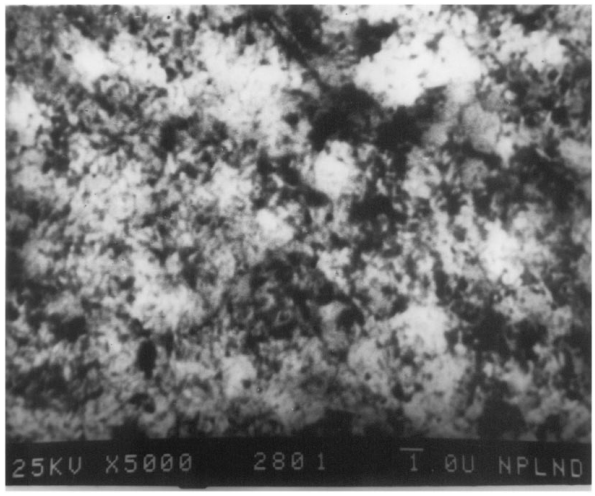

Figure 3 Secondary electron micrograph of a typical copper-rich YBCO thin film. The presence of white lumps may be noticed.

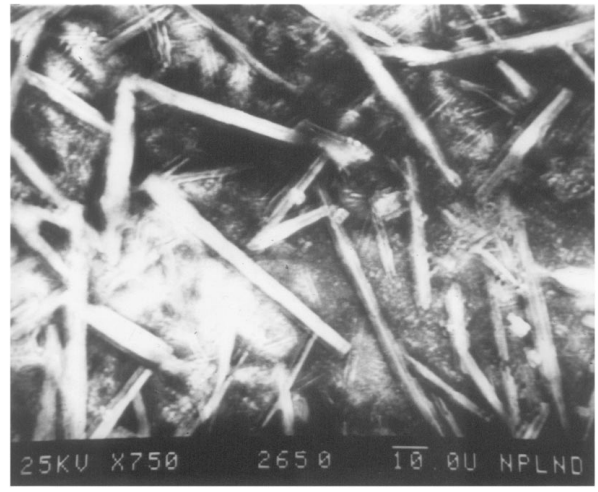

Figure 5 Secondary electron micrograph of YBCO thin film.

3.2. Characterization of thin films

3.2.1. Thin films on $SrTiO_3$ (1 0 0) substrates

Superconducting thin films were prepared on two types of substrate, $SrTiO_3$ (1 0 0) and YSZ (1 0 0) single crystals, under optimized conditions. The deposition and annealing was performed under similar optimized conditions for these two substrates.

The electrical characteristics for all films were taken using the usual four-probe technique. Fig. 4 shows the electrical characteristics of typical YBCO thin films fabricated on $SrTiO_3$ (1 0 0) and YSZ (1 0 0) substrates. The *R-T* characteristics of a YBCO thin film on $SrTiO_3$ substrate having zero resistivity at 85 K are shown in Fig. 4a. A scanning electron micrograph of this thin film is presented in Fig. 5, which shows characteristic long and well-developed bars which are orthogonal to each other. The observation of such morphological structure has been corroborated with other reports in the literature [12]. This well-developed microstructure indicates the possibility of the *c*-axis of the film being normal to the plane of the substrate; this can be corroborated by powder XRD studies. This microstructure also emphasizes near-crystallographic matching of the YBCO film with the substrate $SrTiO_3$ (1 0 0). The difference in the BaF_2 route of YBCO preparation from the technique in which Ba/BaO is used as a source, can be understood by comparison [12] of the microstructures of the samples obtained through both methods. In the BaF_2 route, the film shows large interconnected crystallites of $YBa_2Cu_3O_{7-\delta}$ which are perpendicular to each other, as shown in Fig. 5, while in the barium method, a large number of randomly oriented small grains is observed. The powder X-ray diffraction (XRD) of the samples was performed using the CuK_α line as source. The XRD of this thin film is shown in Fig. 6a. All the peaks are indexed in the light of reported literature [13]. The (0 0 1) peaks are predominantly observed, which indicates that the *c*-axis of the film is perpendicular to the plane of the substrate. This is also supported by microstructural results.

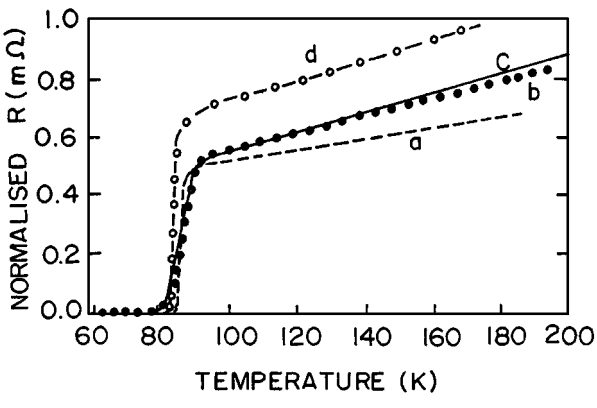

Figure 4 The *R-T* characteristics of YBCO thin films. (a) Y123 on $SrTiO_3$ substrate, (b) Y124 on $SrTiO_3$. (c) *c*-axis-oriented Y124 on $SrTiO_3$. (d) Y123 on YSZ substrate.

3.2.2. Thin films of Y124 phase

There are several reports [14] demonstrating the existence of an ordered defect structure, while studying the X-ray and electron diffraction in epitaxial thin films of YBCO, having an extra copper oxygen layer in every unti cell of the parent 1 : 2 : 3 material. The composition of this defect structure is found to be 2 : 4 : 8. It was understood that changes in growth and post-annealing conditions enable the sample to be made as isolated 1 : 2 : 3 or 2 : 4 : 8 phase or, in a more general case, as faulted structures that mix the two. The rate-limiting step [15] in the formation of YBCO is the conversion of $BaF_2 \rightarrow BaO$ under wet oxygen annealing conditions. The high-temperature annealing step (temperature and duration) can thus influence of formation of $Y_2Ba_1Cu_8O_{16}$ (Y248) or $YBa_2Cu_3O_{7-\delta}$ (Y123) phase. The Y248 phase is also unstable at high temperatures (>850 °C). This gets converted into Y123 phase. Thus, keeping the annealing temperature at 850 °C, and changing the wet-annealing duration (time) it is possible to realize Y248 phase. Fig. 6b shows an XRD of a typical mixed phase (Y123 + Y248) sample annealed at 850 °C for 1 h. All the peaks are indexed [16]. The XRD is dominated by predominantly Y248 phase having two well-developed Y-123 phase peaks, i.e. (0 0 1) and (0 0 2). The scanning electron micrograph (Fig. 7) also exhibits different microstructural growth for both the phases. While one phase leads to bigger platelets, another leads to microcrystallites.

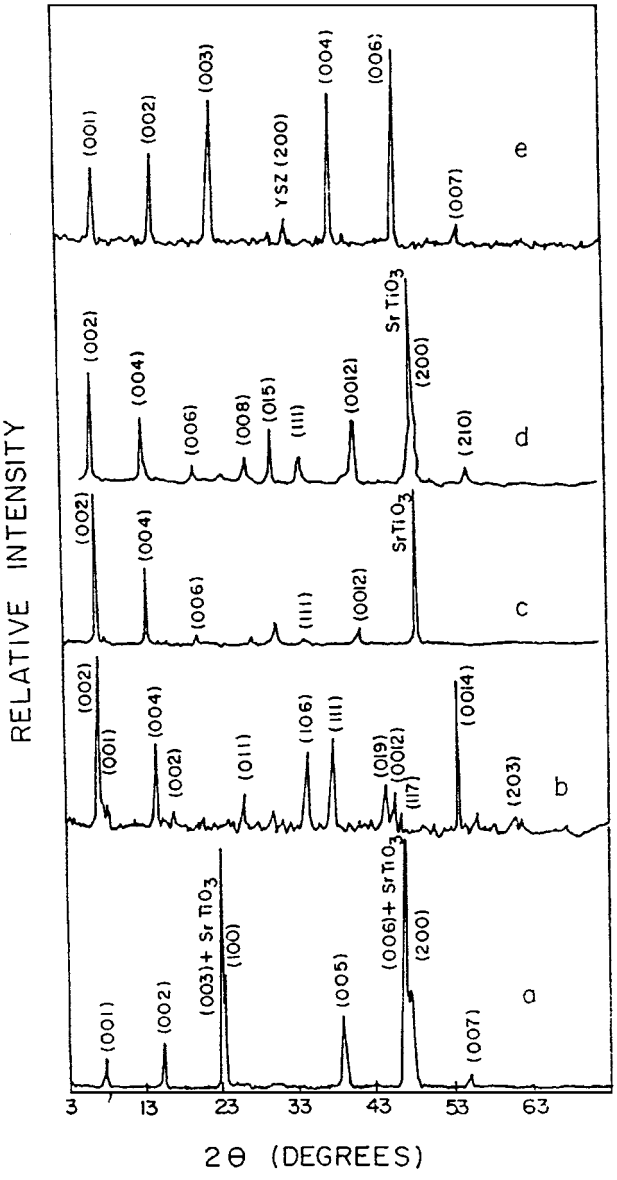

Figure 6 Powder XRD of the YBCO thin films. (a) Y123 phase on $SrTiO_3$ substrate. *c*-axis orientation is apparent from (0 0 1) peaks. (b) Mixed phase (Y123 + Y124) specimen. Note that the starred peaks are Y123 phase and the rest are Y124 phase. (c) *c*-axis oriented Y124 phase. (d) Y123 phase having different orientation of crystallites. (e) Y123 phase on YSZ substrate.

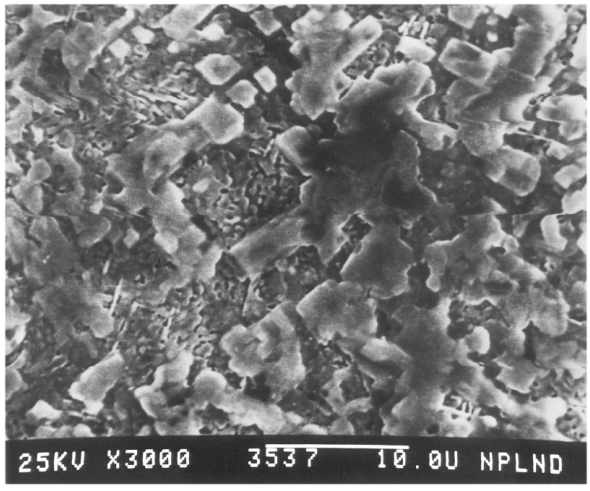

Figure 7 Scanning electron micrograph of a typical mixed-phase YBCO sample. One phase leads to bigger platelets while another leads to microcrystallites.

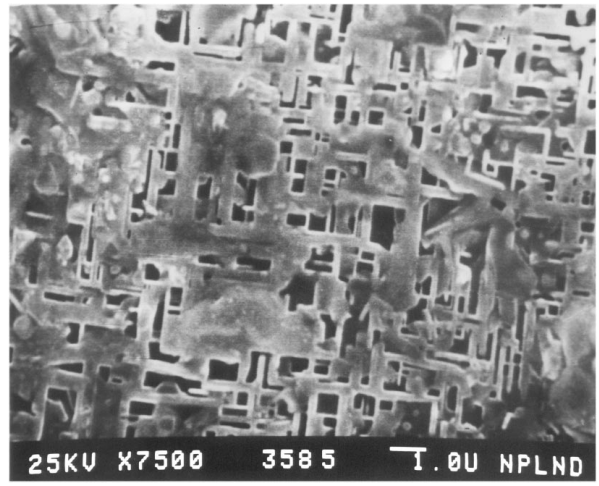

Figure 8 Scanning electron micrograph of Y124 phase. This phase also exhibits a basket-weave structure.

The *R-T* measurement (Fig. 4b) of the sample annealed at 850 °C for 2 h shows it to be superconducting around 80 K. XRD (Fig. 6d) shows it to be polycrystalline Y124 phase. The diffractogram shows peaks corresponding to (0 0 1) and also peaks corresponding to different orientations (0 1 5), (1 1 1) and (2 1 0). The absence of Y123 phase can readily be observed. The sample annealed at 850 °C for 3 h in wet oxygen conditions, even though it shows superconductivity around 80 K (Fig. 4c), has superior crystallite orientations, as revealed by powder XRD (Fig. 6c). The XRD exhibits Y248 phase having all (0 0 1) peaks. So it can be understood that growth of Y248 phase proceeded with its *c*-axis oriented perpendicular to the plane of the substrate. The scanning electron micrograph (Fig. 8) shows the microstructure of pure Y248 phase. It is evident that this phase also displays a basket-weave like structure. Comparing the *R-T* characteristics of polycrystalline and *c*-axis-oriented Y124, it can be understood that the transition width of the *c*-axis oriented Y124 specimen is lower.

3.2.3. YBCO thin films on YSZ (1 0 0) substrates

The YBCO superconducting thin films are fabricated on yttria-stabilized zirconia (YSZ) single-crystal substrates with similar growth and annealing conditions to those observed with $SrTiO_3$ (1 0 0) substrates.

Fig. 4d shows the variation of resistance with temperature (*R-T*) for a typical YBCO thin film on YSZ substrates. The *R-T* characteristics of the specimen show the thin film to be superconducting around 80 K, while the XRD (Fig. 6e) reveals the *c*-axis-oriented growth of the thin film. The scanning electron micrograph (Fig. 9) shows the pebble-like morphology consistent with the XRD results.

3.2.4. Comparison of microstructures on $SrTiO_3$ (1 0 0) and YSZ (1 0 0) substrates

The microstructure of superconducting Y123 phase on $SrTiO_3$ (1 0 0) and on YSZ (1 0 0) reveal interesting comparisons. Both the substrates facilitate strong

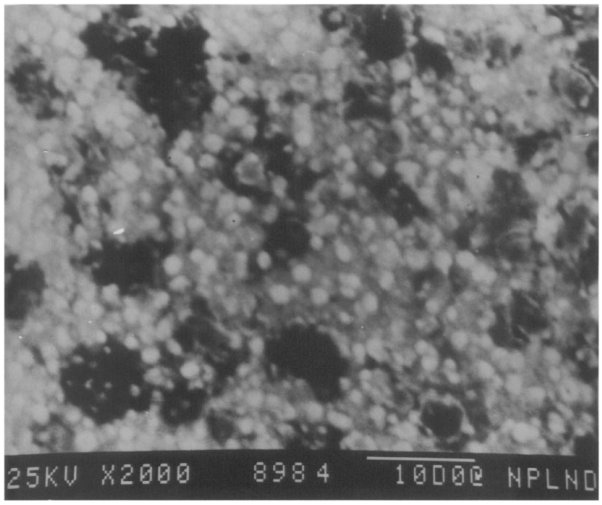

Figure 9 Scanning electron micrograph of a typical Y123 thin film on YSZ (1 0 0) substrate. The pebble-like structure can be observed.

c-axis-oriented growth. However, the growth morphology is quite different in the two cases. While Y123 phase on $SrTiO_3$ exhibits long bars orthogonal to each other and have well-developed junctions, the microstructure on YSZ substrate reveals growth of a simple crystalline (pebble-like) structure. The differences in the microstructures may be understood in terms of lattice matching and also matching of the thermal expansions of the substrates with that of YBCO. It is now well understood that $SrTiO_3$ (1 0 0) substrates are more suitable for YBCO thin-film growth. In YBCO there are four [17] crystallographically inequivalent (0 0 1) layers that can interfacially bond with the YSZ surface. Through simulations of structural interfaces at an atomic level, it is known that out of these four planes, three are observed to initiate at the surfaces of various substrates. On $SrTiO_3$, the CuO plane forms the interface [18]. Owing to large lattice mismatch between YBCO and YSZ substrate, three main epitaxial orientations have been observed [17] for *c*-axis films on YSZ. These can be understood to arise from the different YBCO unit cell layers which initiate the interfacial configurations. Thus the growth modes of the thin films of $SrTiO_3$ (1 0 0) and YSZ (1 0 0) substrates differ from each other.

4. Conclusion

By following the BaF_2 route, it is possible to fabricate pure Y124 phase which, at high temperatures, transforms to pure Y123 phase. Incomplete transformation leads to faulted structures having mixed phases (Y123 + Y124). Optimized conditions of annealing in the case of Y123 on $SrTiO_3$, give optimum stoichiometry, bigger bar-like microstructures, *c*-axis-oriented crystallites and superconducting T_c around 85 K. The Y124 phase also exhibits a basket-weave structure similar to that of Y123. The off-stoichiometry has deleterious effects on microstructure and superconducting properties.

Acknowledgements

Thanks are due to Professor E. S. R. Gopal, Director, for permission to publish this work. The authors are grateful to Dr D. K. Suri and Dr R. P. Pant for their help in carrying out XRD studies, and Dr S. U. M. Rao for SEM measurements. One of the authors (V.H.S.) thanks the Department of Atomic Energy, Government of India, for awarding a Dr K. S. Krishnan Research fellowship and the Indo-French Centre for Promotion of Advanced Research, for their partial financial support.

References

1. V. MATIJASEVIC, P. ROSENTHAL, K. SHINOHARA, A. F. MARSHALL, R. H. HAMMOND and M. R. BEASLEY, *J. Mater. Res.* **6** (1991) 682.
2. D. BHATT, S. N. BASU, A. C. WESTERHEIM and A. C. ANDERSON, *Physica C* **222** (1994) 283.
3. Applied Surface Science 96-98 (1996): Proceedings of Symposium F: Third International Conference on Laser Ablation of the 1995 E-MRS Spring Conference, Strasburg, France (1995).
4. B. C. RICHARDS, S. L. COOK, D. L. PINCH, G. W. ANDREWS, G. LENGELING, B. SCHULTE, H. JURGENSEN, Y. Q. SHEN, P. VASE, T. FRELOFT, C. I. M. A. SPEE, J. L. LENDEN, M. L. HITCHMAN and A. BROWN, *Physica C* **252** (1995) 229.
5. P. M. MANKIEWICH, J. H. SCOFIELD, W. J. SKOCPOL, R. E. HOWARD, A. H. DAYEM and E. GOOD, *Appl. Phys. Lett.* **51** (1987) 1753.
6. D. J. CARLSON, M. P. SIEGAL, J. M. PHILLIPS, T. H. TIEFEL and J. H. MARSHALL, *J. Mater. Res.* **5** (1990) 2797.
7. J. M. PHILLIPS, *J. Appl. Phys.* **79** (1996) 1829.
8. IL 400 Deposition Controller (Intellemetrics) Instruction Manual Version 4.7/4.0.
9. MICHAEL P. SEIGAL, JULIA M. PHILLIPS, R. B. VAN DOVER, T. H. TIEFEL and J. H. MARSHALL, *J. Appl. Phys.* **68** (1990) 6353.
10. B. SCHULTE, M. MAUL, P. HAUSSLER and H. ADRIN, *Appl. Phys. Lett.* **62** (1993) 633.
11. R. S. ROTH, C. J. RAWN, F. BEECH, J. D. WHITLER and J. O. ANDERSON, in "Ceramic Superconductors II," edited by M. F. Yan (The American Ceramic Society, Westerville, OH, 1988) p. 303.
12. V. G. VAZQUEZ and C. M. FALCO, *Mater. Res. Symp. Proc.* **169** (1990) 683.
13. S. Y. HOU, J. M. PHILLIPS, D. J. WERDER, T. H. TIEFEL, R. M. FLEMING, J. H. MARSHALL and M. P. SIEGAL, *Appl. Phys. Lett.* **62** (1993) 3201.
14. R. L. BURTON, C. U. SEGRE, H. O. MARCY and C. R. KANNEWURF, in "Science and Technology of Thin Film Superconductors," edited by R. D. McConnel and S. A. Wolf (Plenum Press, New York, 1989) p. 61.
15. A. M. T. BELL, *Supercond. Sci. Technol.* **3** (1990) 55.
16. K. CHAR, MARK LEE, R. W. BARTON, A. F. MARSHALL, I. BOZOVIC, R. H. HAMMOND, M. R. BEASLEY, T. H. GEBALLE, A. KAPITULNIK and S. S. LADERMAN, *Phys. Rev. B* **38** (1988) 834.
17. R. RAMESH, D. M. HWANG, T. VENKATESAN, T. S. RAVI, L. NAZAR, A. INAM, X. D. WU, B. DUTTA, G. THOMAS, A. F. MARSHALL and T. H. GEBALLE, *Science* **247** (1990) 57.
18. F. H. GARZON, J. G. BEERY, D. R. BROWN, R. J. SHERMAN and I. D. RAISTRICK, *Appl. Phys. Lett.* **54** (1989) 1365.
19. A. KAPITILNIK and K. CHAR, *IBM J. Res. Develop.* **33** (1989) 252.
20. J. MACMANUS-DRISCOLL, T. H. GEBALLE and J. C. BRAVMAN, *J. Appl. Phys.* **75** (1994) 412.
21. R. RAMESH, A. INAM, D. M. HWANG, T. S. RAVI, T. SANDS, X. X. XI, X. D. WU, Q. II, T. VENKATESAN and R. KILAAS, *J. Mater. Res.* **6** (1991) 2264.

Received 7 April 1997
and accepted 22 April 1998